



Galectin-1 in injured rat spinal cord: Implications for macrophage phagocytosis and neural repair



Andrew D. Gaudet^{*}, David R. Sweet¹, Nicole K. Polinski², Zhen Guan, Phillip G. Popovich^{*}

Center for Brain and Spinal Cord Repair, The Ohio State University, Room 670, Biomedical Research Tower, 460W, 12th Ave., Columbus, OH 43210, USA
Department of Neuroscience, Wexner Medical Center, The Ohio State University, Room 670, Biomedical Research Tower, 460W, 12th Ave., Columbus, OH 43210, USA

ARTICLE INFO

Article history:

Received 15 August 2014
Revised 30 October 2014
Accepted 22 December 2014
Available online 24 December 2014

Keywords:

Spinal cord injury
Neuroinflammation
Inflammation
Glial scar
Phagocytosis
Extracellular matrix

ABSTRACT

Galectin (Gal)-1 is a small carbohydrate-binding protein and immune modulatory cytokine that is synthesized locally at the site of peripheral nerve injury. In this environment, Gal1 can promote regeneration of injured peripheral axons, in part by modifying the function of macrophages recruited to the site of injury. Unlike in injured peripheral nerves, macrophages do not promote axon regeneration in the injured central nervous system (CNS), perhaps because Gal1 levels are not regulated appropriately. Because the dynamics and cellular localization of endogenous Gal1 have not been rigorously characterized after CNS injury, we examined the spatio-temporal distribution of Gal1 in rat spinal cords subjected to a standardized contusion injury. Whereas Gal1 was not expressed in uninjured spinal cord, it was significantly upregulated after SCI, especially within the lesion core. Gal1 was expressed in ~40% of lesion-localized macrophages at 3–28 days post-injury (dpi), and in ~45% of astrocytes in the lesion border at 7–28 dpi. Most lesion-localized Gal1 + macrophages did not express the phagocytosis marker ED1, and Gal1 + cells contained less phagocytosed lipids. These data suggest that time- and location-dependent regulation of Gal1 by macrophages (and astrocytes) could be important for modulating phagocytosis, inflammation/gliosis, and axon growth after SCI.

© 2014 Elsevier Inc. All rights reserved.

1. Introduction

Galectin-1 (Gal1) is a 14.5 kDa carbohydrate-binding protein (lectin) that promotes regeneration of injured peripheral nervous system (PNS) axons (Gaudet et al., 2005, 2011; McGraw et al., 2004a, 2004b, 2005; Rabinovich et al., 2007). Gal1 enhances PNS regeneration indirectly by acting on non-neuronal cells, particularly macrophages (Horie et al., 2004). Gal1 function is controlled by redox state: when oxidized, Gal1 is a monomer that has little lectin activity and acts similar to a cytokine (as opposed to the dimeric reduced form) (Inagaki et al., 2000). Oxidized Gal1 likely drives axon regrowth by regulating macrophage inflammatory signaling, accumulation, and phagocytosis (Echigo et al., 2010; Gaudet et al., 2009; Horie et al., 2004).

Abbreviations: BDNF, brain-derived neurotrophic factor; CNS, central nervous system; ECM, extracellular matrix; Gal1, galectin-1; GFAP, glial fibrillary acidic protein; –IR, –immunoreactivity; PNS, peripheral nervous system; SCI, spinal cord injury

^{*} Corresponding authors at: Center for Brain and Spinal Cord Repair, The Ohio State University, Room 670, Biomedical Research Tower, 460W, 12th Ave., Columbus, OH 43210, USA.

E-mail addresses: gaudet.6@osu.edu (A.D. Gaudet), popovich.2@osu.edu (P.G. Popovich).

¹ Current address: School of Medicine, Case Western Reserve University, Cleveland, OH, USA.

² Current address: Translational Science and Molecular Medicine, Michigan State University, Grand Rapids, MI, USA.

After spinal cord injury (SCI), blood monocytes infiltrate the lesion site then differentiate into inflammatory (M1) macrophages that can exacerbate pathology (secondary damage) (Donnelly and Popovich, 2008; Kigerl et al., 2009). In contrast to macrophages that respond to peripheral tissue damage, inflammatory macrophages in SCI lesions do not phagocytose efficiently and these cells persist indefinitely at sites of injury (Gaudet et al., 2011; Greenhalgh and David, 2014; Herbert et al., 2004; Kigerl et al., 2009; Martinez et al., 2009; Martini et al., 2008; Mosser and Edwards, 2008). These features of CNS macrophages have been implicated in regeneration failure after SCI (McPhail et al., 2004; Pruss et al., 2011; Stirling et al., 2004; Vallieres et al., 2006).

Data from animal models indicate that Gal1 could influence recovery after SCI. Exogenous Gal1 may improve recovery after SCI in mice, possibly through altering astrocyte physiology (Han et al., 2011) or improving axon plasticity (Quinta et al., 2014). Transplantation of Gal1-expressing neural stem cells also improves anatomical and behavioral recovery after SCI in marmosets (Yamane et al., 2010). In these latter studies, Gal1 was added to the injured spinal cord, suggesting that the spatiotemporal regulation of endogenous Gal1 after SCI is not optimal for regulating inflammation or creating a growth permissive environment. Indeed, Gal1 is expressed at low levels in the uninjured adult CNS (Akazawa et al., 2004). Rubrospinal neurons, which do not mount an effective regenerative response, fail to upregulate Gal1 at two weeks post-SCI (McGraw et al., 2004b).

Here, we perform the first comprehensive quantitative analysis of Gal1 expression and cellular localization after SCI. We show that Gal1 mRNA and protein increase significantly in the lesion epicenter during the first week post-SCI with persistent expression evident in cells within and adjacent to the injury site. In the lesion core, Gal1 is upregulated in macrophages/microglia, mainly those that are non-phagocytic (OX42 +/ED1 –). The inverse relationship between expression of Gal1 and ED1 (a lysosome associated protein) corresponded with fewer Gal1 + cells containing phagocytosed lipids at the peak of the inflammatory response (at 14 dpi). In the lesion border, Gal1 is not significantly elevated in microglia; rather, Gal1 is increased in reactive astrocytes of the glial scar. These data suggest that time- and location-dependent regulation of Gal1 by macrophages (and astrocytes) could be important for modulating phagocytosis, inflammation/gliosis, and axon growth after SCI.

2. Results

2.1. Galectin-1 mRNA and protein are upregulated transiently at the SCI epicenter

To determine how Gal1 mRNA and protein expression change after SCI, spinal cord segments were isolated from naïve, sham, or SCI rats at different times post-injury. Gal1 mRNA expression was significantly increased in the lesion epicenter at 3 days post-injury (dpi) (203% higher than uninjured; Fig. 1a). Gal1 protein exists in an equilibrium between monomeric and dimeric forms. Both Gal1 types increased after SCI (Fig. 1b); dimeric Gal1 increased 360% at 7 dpi, whereas monomeric Gal1 was increased at 7 and 14 dpi compared to uninjured control tissue (270% and 360% higher than uninjured, respectively). Therefore, a monophasic increase in expression of both Gal1 mRNA and protein occurs at the lesion epicenter between 7 and 14 d post-SCI.

2.2. Galectin-1 increases in cells and matrix surrounding the spinal contusion lesion

Immunohistochemistry was used to document the temporal and spatial distribution of Gal1 immunoreactivity (IR) in cells throughout intact and injured spinal cord (Fig. 2). Compared with uninjured spinal cord (Fig. 2k), Gal1-IR increased significantly in lesioned tissue by 7 dpi (Fig. 2a–e, l) then continued to increase throughout the rostro-caudal extent of the lesion until 14 dpi (Fig. 2l) after which Gal1-IR decreased toward baseline/uninjured control levels at 28 dpi (Fig. 2f–j, l). Gal1-IR was significantly increased in cells and tissue directly adjacent to the lesion (glial scar) at all timepoints (Fig. 2i (inset), m, n).

In uninjured spinal cords, primary afferent terminals in the superficial dorsal horn, motor neurons in the ventral horn and axons throughout the white matter were Gal1-IR (Fig. 3a'–d'). By 7 dpi, most Gal1-IR was found in inflammatory cells, predominantly macrophages (Fig. 3e'–h'), although Gal1-IR also increased in fusiform cells, presumably astrocytes (arrowheads, Fig. 3f', f''; see also Fig. 5), nearby the lesion and in central canal ependyma (arrows, Fig. 3g', g'').

2.3. Galectin-1 immunoreactivity is increased and sustained in a subset of macrophages/microglia within the lesion epicenter

Although Gal1 was undetectable in microglia in the uninjured spinal cord (Fig. 4a, b), Gal-IR increased markedly in activated OX42 + macrophages/microglia after SCI (Fig. 4c–j). A high density of Gal1-IR cells was found in the lesion epicenter at all timepoints examined. To quantify Gal1 expression in lesion-localized macrophages/microglia, OX42 + cells within the lesion epicenter were circled, then area and average Gal1-IR intensity per macrophage were quantified. The OX42 antibody recognizes CD11b/c (Tamani et al., 1991). Compared with microglia in uninjured tissue, macrophages/microglia in the lesion had significantly higher average Gal1-IR intensity at all timepoints (Fig. 4k, l).

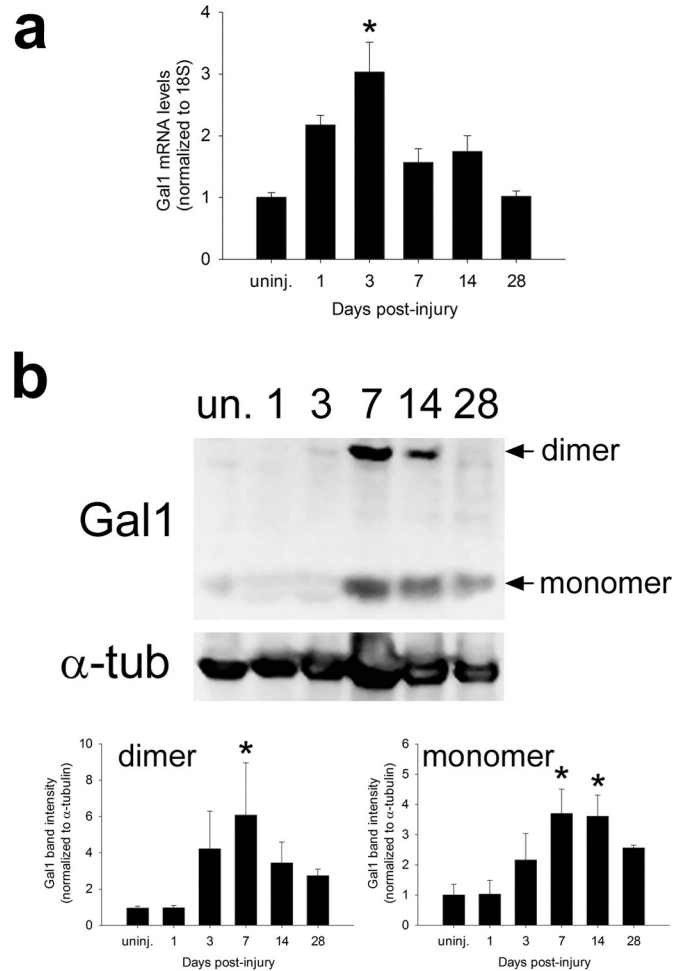


Fig. 1. Gal1 mRNA and protein increased in the lesion epicenter after moderate SCI. (a) Gal1 mRNA levels, assessed using qRT-PCR, increased 200% at 3 dpi compared to uninjured spinal cord. (b) Gal1 protein, assessed using Western blots, also increased after SCI: Gal1 dimer (~29 kDa) increased significantly at 7 dpi, while expression of Gal1 monomer (14.5 kDa) increased at 7 and 14 dpi compared to uninjured spinal cord. Gal1 bands were normalized to α -tubulin (α -tub) expression; uninj (uninjured). * $p < 0.05$ vs. uninjured.

Although macrophage density and size changed over time (macrophages in 3 dpi lesions were more sparsely distributed and smaller than those at later times), 30–40% of macrophages were Gal1 + at all post-injury timepoints examined (compared to 1.2% of microglia in uninjured spinal cord). At later times post-injury (14, 28 dpi), Gal1-IR was reduced and more diffuse in large multi-nucleated macrophages with phagocytic inclusions (Fig. 4g–j). These data indicate that activated macrophages/microglia in the lesion express higher levels of Gal1 than do parenchymal microglia, and that the proportion of Gal1 + macrophages in the lesion remains constant between 3–28 dpi.

2.4. Astrocytes, but not microglia, express galectin-1 in the lesion border

As shown in Fig. 1, Gal1-IR was increased in cells in the glial scar. Confocal microscopy was used to reveal the identity of Gal1-expressing cells in the penumbral tissue (Fig. 5). OX42 + parenchymal microglia, even those closer to the lesion, express low levels of Gal1 (Fig. 5a–f, m). Conversely, OX42 + cells associated with blood vessels, presumably perivascular microglia or newly recruited monocytes, were Gal1 + (asterisk, Fig. 5d–f). Overall, Gal1-IR in glial scar OX42 + cells was significantly lower than in lesion-localized microglia/macrophages (Fig. 5m).

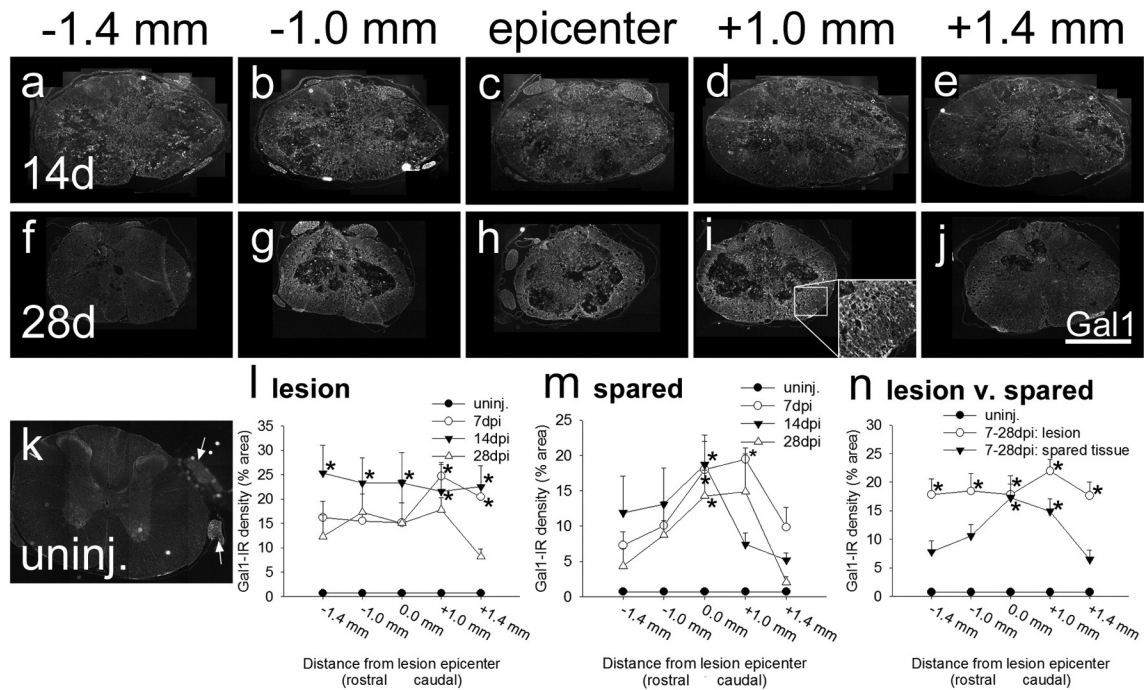


Fig. 2. Gal1-IR is increased in lesioned and spared tissue after SCI. Images of spinal cord collected from animals at various survival times (a–k) were analyzed for density of Gal1-immunoreactivity (IR) (l–m). In uninjured spinal cord (k), Gal1-IR was found mainly in primary afferent terminals in the dorsal horn and in ventral horn motor neurons (note also Gal1-IR in connected dorsal and ventral roots; arrows). At the lesion site (l), Gal1-IR increased at 7 and 14 dpi compared to uninjured tissue. In spared tissue (m), Gal1-IR was significantly increased at the rostro-caudal lesion epicenter, with a progressive decrease in Gal1-IR moving away from the epicenter. This represented a higher proportional contribution of the glial scar to Gal1-IR in the epicenter. When data were collapsed across all timepoints (n), Gal1-IR was consistently higher in epicenter-localized cells compared to uninjured control and spared tissue. * $p < 0.05$ vs. uninjured. Scale bar = 1 mm.

Most Gal1-IR cells in the scar had an astrocyte-like morphology (Fig. 5g–l). In uninjured tissue, 4.5% of GFAP+ cells were Gal1-IR; however, by 7–28 dpi, 40–50% of GFAP+ astrocytes showed increased expression of Gal1 (Fig. 5n). Therefore, astrocytes, but not microglia, preferentially upregulate expression of Gal1 in the glial scar.

2.5. Gal1 may regulate phagocytosis after SCI

Within the lesion epicenter, large lipid-laden macrophages expressed low levels of Gal1 compared with smaller macrophages/microglia, suggesting that a cell's phagocytic potential might vary inversely with Gal1 expression. Therefore, the ratio of microglia/macrophages that co-labeled with anti-Gal1 and ED1 antibodies was quantified. The ED1 antibody labels CD68, a 110-kDa transmembrane glycoprotein that contains a lysosome associated membrane protein-like domain; the relative amount of ED1 correlates with phagocytic activity (Damoiseaux et al., 1994; Holness and Simmons, 1993).

As expected, no ED1+ cells were observed in uninjured spinal cord (Fig. 6a–c). ED1+ cells were found in the lesion core by 3 dpi, which coincides with initial infiltration of monocyte-derived macrophages (Popovich et al., 1997) and increased Gal1-IR (see Fig. 4). At 3 dpi, many Gal1+ cells also expressed ED1 (56%; Fig. 6d–f, p). Despite maintained Gal1 expression in ~35% of macrophages through 28 dpi (see Fig. 4), fewer Gal1+ macrophages co-expressed ED1 after 7 dpi (17–25%; Fig. 6g–o, p). (See the yellow portion in Fig. 6q, which represents the Gal1+/ED1+ cell population that shrinks after 3 dpi.) Interestingly, at 7 dpi and later, a subset of large Gal1+/ED1– macrophages contained ED1+ intracellular compartments, presumably phagolysosomes (Fig. 6o). In the lesion border, ED1+ cells were all Gal1-negative.

To further characterize the relationship between Gal1, ED1, and phagocytosis, sections were stained to reveal colocalization of Gal1 with Oil Red O (ORO) (Fig. 7). ORO stains lipids derived from myelin and other cellular debris that accumulate within phagocytic macrophages. ORO was found in few macrophages at 3 dpi (Fig. 7d–f), but it

was prevalent in macrophages beginning at 7 dpi (Fig. 7g–i) with ORO+ macrophages persisting in chronic lesions (Fig. 7r–t). To study the relationship between Gal1 expression and ORO accumulation in individual macrophages, we performed linear regression. In lesion-localized macrophages at 14 dpi, the intensity of Gal1 expression was negatively correlated with ORO density (Fig. 7q). These data indicate that intracellular Gal1 may be inversely related with macrophage phagocytic potential.

3. Discussion

To our knowledge, this is the first comprehensive examination of the spatio-temporal regulation of Gal1 in a model of spinal contusion injury. Previous studies were qualitative and more restricted in the scope of their anatomical analyses (Han et al., 2011; Kurihara et al., 2010). Here, we explored constitutive and SCI-induced expression of Gal1 in rats subjected to a standardized spinal contusion injury. Gal1 mRNA and protein increased during the first week post-injury. Most Gal1-IR was present within cells in the injury epicenter and cells/matrix of the glial scar. In normal spinal cord, microglia and astrocytes did not express Gal1, as assessed by immunofluorescent double-labeling. However, after SCI both cell types increased Gal1 expression with distinct spatio-temporal patterns relative to the injury epicenter. In the lesion core at 7–28 dpi, ~40% of macrophages were Gal1+; in contrast, few penumbral microglia were Gal1+. Most lesion-localized Gal1+ macrophages were ED1-negative, suggesting a possible association between Gal1 expression and phagocytic capacity. Indeed, compared to Gal1-negative cells, lipid phagocytosis was reduced in Gal1+ macrophages at 14 dpi. Astrocytes were not found in the injury epicenter, but were present in the adjacent glial scar. Here, ~40–50% of GFAP+ astrocytes were Gal1+. Our data indicate that expression of Gal1 increases in macrophages and astrocytes early after SCI. Although the functional significance of this de novo expression is not known, Gal1 could act as an autocrine/paracrine regulator of inflammation, gliosis, and CNS repair.

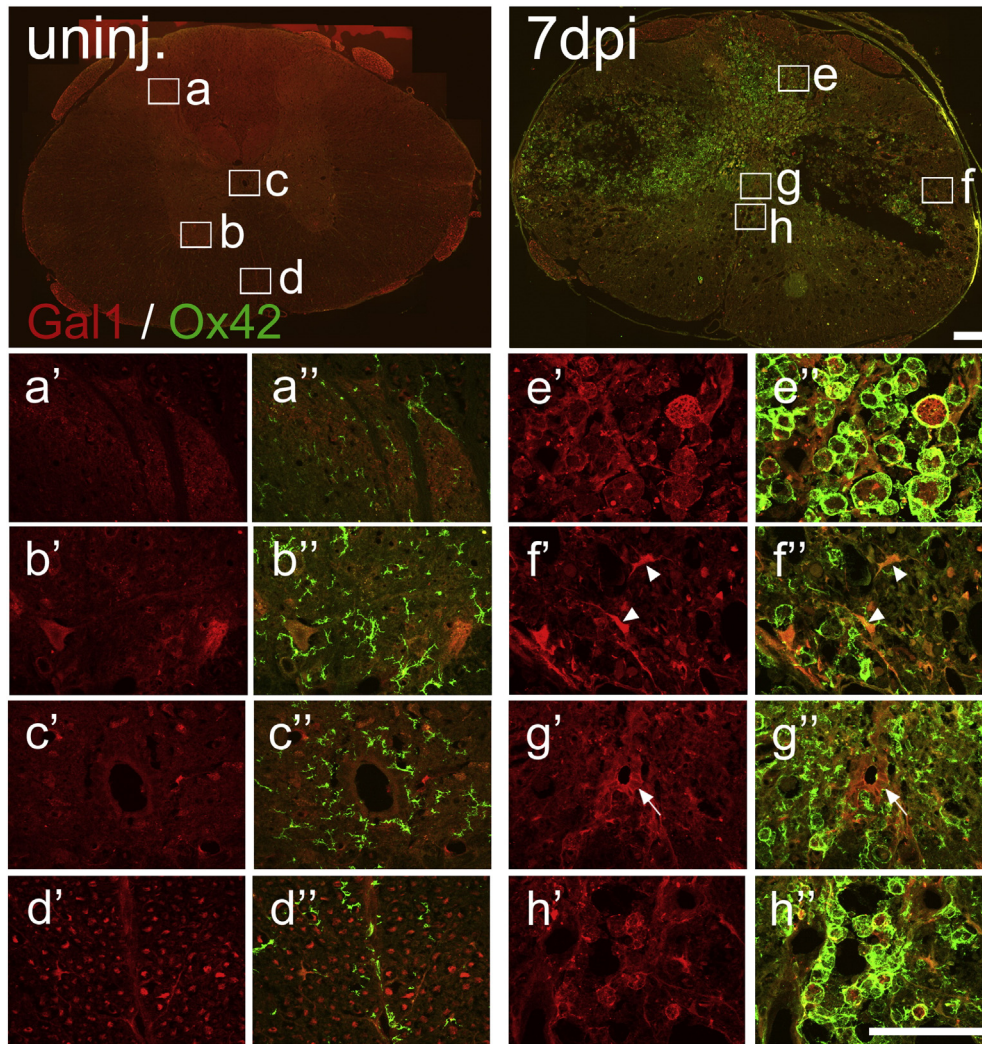


Fig. 3. Localization and cell specificity of SCI-induced Gal1 expression. Boxed regions (a–h) in low power images of uninjured (uninj.) or 7 dpi spinal cord cross-sections represent areas where higher magnification confocal images (a'–h' and a''–h'') were taken. All sections were double-labeled for Gal1 (red) and microglia (OX42, green) and merged images are shown in a''–h''. Gal1-IR was relatively low in uninjured spinal cord; it was expressed in primary afferent terminals in superficial dorsal horn laminae (a, a', a''), a subset of motor neurons in ventral horn (b, b', b''), presumed glia nearby central canal (c, c', c''), and some ventral white matter axons (d, d'). Resident microglia did not express Gal1 in uninjured spinal cord (a'–d''). At 7 dpi, lesion-localized OX42+ macrophages (e, e', e'') were highly Gal1-IR. In spared tissue adjacent to the lesion, Gal1-IR was expressed strongly in fusiform cells (arrowheads; f, f', f''), but not microglia. Gal1 was also increased in cells of the central canal (arrow; g, g', g'') and by macrophages abutting the ventral sulcus (h, h', h''). 7 dpi cross-section was taken 1.6 mm caudal to the lesion epicenter. Scale bars = 100 μ m. (For interpretation of the references to color in this figure legend, the reader is referred to the web version of this article.)

3.1. Potential impact of Gal1 after SCI: is galectin-1 good for the environment?

The inverse relationship between Gal1 and phagocytic markers at the injury epicenter during the time of maximal post-injury inflammation (7–28 dpi) could implicate Gal1 in regulation of post-injury phagocytosis. Using human monocytes, Barrionuevo et al. (2007) found that Gal1 differentially regulated constitutive and inflammatory-induced phagocytosis: Gal1 addition alone for 24 h increased Fc γ R-dependent erythrocyte phagocytosis, whereas Gal1 co-treatment reduced phagocytosis when applied in the context of IFN- γ signaling. Interestingly, phagocytic activity also was increased in Gal1 null mutant macrophages, suggesting that intracellular Gal1 could dampen phagocytosis. Since most macrophages in the injury epicenter exhibit an inflammatory phenotype (Kigerl et al., 2009), increasing intracellular and/or extracellular Gal1 could limit their phagocytic potential.

Previous studies showed that Gal1 can reduce inflammatory signaling in macrophages and may promote their differentiation into a reparative phenotype. For example, Gal1 mitigates nitric oxide production and favors arginase synthesis. This change in arginine metabolism is a

hallmark characteristic of alternative (M2) macrophage activation and has been linked with tissue repair within and outside the CNS (Correa et al., 2003; Echigo et al., 2010; Lee et al., 2011; Miron et al., 2013; Pesce et al., 2009; Thomas et al., 2007). This may explain why injections of Gal1 suppress rat hind paw inflammation/edema following intradermal injection of phospholipase-A2 (Rabinovich et al., 2000), an enzyme that hydrolyzes phospholipids creating a pool of inflammatory mediators. Since Gal1 can enhance formation of an M2 macrophage phenotype, especially in the presence of persistent inflammatory signals after SCI, the post-injury increase in Gal1 expression could represent an intrinsic attempt by macrophages and astrocytes to limit inflammation and restore homeostasis. As this endogenous response is insufficient, introducing exogenous Gal1 after SCI might represent a novel anti-inflammatory or neuroprotective intervention.

SCI-induced Gal1 upregulation in astrocytes could also play a key role in tissue repair and remodeling. Gal1 is expressed at low levels in astrocytes in the uninjured spinal cord; however, Gal1 is present in a higher proportion (40–50%) of GFAP+ cells/processes from 7–28 dpi (Fig. 5). Previous studies showed that cultured astrocytes express and secrete Gal1 (Qu et al., 2010; Yin et al., 2012). Similarly, Gal1 is

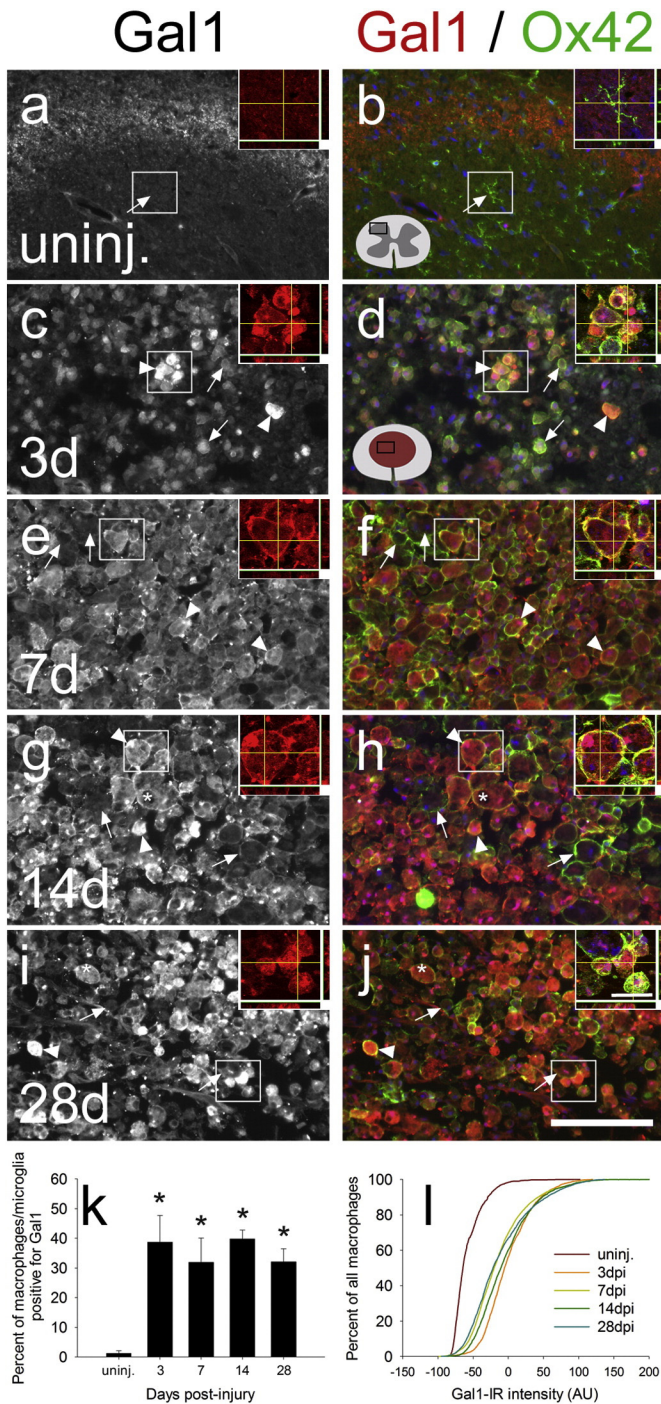


Fig. 4. Gal1 expression was increased in lesion-localized macrophages/microglia after SCI. Gal1-IR is shown in the left images; Gal1/Ox-42 merged images are shown on the right. Arrows identify examples of Gal1⁺/Ox42⁺ cells; arrowheads delineate Gal1⁺/Ox42⁺ cells. (a, b) Gal1-IR was relatively low in resident Ox-42-IR microglia (here shown in the dorsal horn). (c–j) After SCI, a subset of macrophages in the lesion epicenter expressed Gal1. At 7–28 dpi, larger Ox42⁺ macrophages often colocalized with diffuse Gal1-IR (see asterisks in g–j). (k) At all post-injury timepoints, 30–40% of Ox42⁺ macrophages expressed Gal1, which is significantly higher than the ~1% of microglia that were Gal1⁺ in uninjured spinal cord. (l) Despite major differences in macrophage density, size, and phenotype, no significant shift in the distribution of Gal1-IR within the macrophage population was observed between post-injury timepoints. In the cumulative distribution, a rightward shift represents higher Gal1-IR; 0 on the x-axis represents the threshold for Gal1 positivity. **p* < 0.05. Scale bars = 100 μ m (large images), 25 μ m (insets).

upregulated in GFAP⁺ cells in animal models of multiple sclerosis and cerebral ischemia (Qu et al., 2010; Stancic et al., 2011). Gal1-treated astrocytes show decreased proliferation and increased brain-derived

neurotrophic factor (BDNF) secretion (Sasaki et al., 2004). These effects may underlie Gal1's beneficial therapeutic outcomes in ischemia models where Gal1 treatment was associated with increased BDNF and decreased reactive astrogliosis (Ishibashi et al., 2007; Qu et al., 2011; Qu et al., 2010). Therefore, endogenous Gal1 may limit SCI-induced gliosis and promote trophic factor release. We found increased Gal1-IR in the extracellular matrix (ECM) near the injury epicenter. This increase was evident only after the lesion and scar had consolidated, forming a visibly robust boundary between the lesion core and spared tissue. Thus, endogenous Gal1 may not inhibit scarring after SCI, but the protein could have other functions within the scar. Gal1 can bind specific chondroitin sulfates (Moiseeva et al., 2003) and other ECM molecules that exist after SCI (Camby et al., 2006). Therefore, Gal1 released by astrocytes and macrophages could bind glial scar ECM molecules, which could immobilize Gal1 to create an anti-inflammatory "net" that alters the physiology, adhesion, and mobility of nearby cells.

Reduced galectin-1 (dimer), has lectin activity, is upregulated in degenerating neurons, and can cause neuronal degeneration (Plachta et al., 2007). Conversely, oxidized galectin-1 (monomer), lacks lectin activity, promotes neurite outgrowth, and enhances peripheral axonal regeneration, in part by stimulating growth factor release from macrophages (Outenreath and Jones, 1992; Inagaki et al., 2000; Fukaya et al., 2003; Horie et al., 2004). Although the antibody used in the current study does not discriminate between monomeric or dimeric forms of Gal1 using immunohistochemistry, Western blot data indicate that Gal1 exists primarily as a monomer early after SCI. The early accumulation of monomeric Gal1 could result from the rapid accumulation of oxidative metabolites that are released within 30 min post-SCI that then persist for days within the lesion and in proximal/distal segments of spinal cord (Liu et al., 2013; Carrico et al., 2009). However, at later post-injury times (e.g., > 14 d) when oxidative stress dissipates, monomeric and dimeric Gal1 may equilibrate. Again, Western blot data confirm this equilibration. Our current data identify discrete spatiotemporal patterns of Gal1 expression and suggest that manipulating the oxidation state of Gal1 at later times post-injury could help enhance spinal cord repair.

4. Conclusions

Although previous studies have described SCI-induced changes in Gal1 expression, including co-localization of Gal1 with astrocytes and inflammatory cells, our current report is the first to quantitatively document the spatio-temporal regulation of Gal1 in a model of spinal contusion injury. In a mouse model of dorsal spinal hemisection injury, Kurihara et al. (2010) found that Gal1 co-localized with markers for neutrophils (myeloperoxidase), macrophages (Iba1), and astrocytes (GFAP). These analyses were qualitative and were restricted to the first 7 days post-injury without reference to whether Gal1 expression was changing in the frank lesion, penumbra, or distal spinal cord. Han et al. (2011) also described an increase in Gal1-expressing astrocytes in the contused mouse spinal cord, but without quantifying these changes over time or with respect to injury location. Our data significantly extend these previous reports by systematically describing changes in Gal1 expression over extended post-injury intervals and with respect to discrete regions and cell types throughout the injured spinal cord. Such details will help refine the therapeutic window for future studies that attempt to manipulate Gal1 expression.

The robust SCI-induced upregulation of Gal1 in lesion-localized macrophages and in astrocytes and ECM near the injury epicenter suggests that Gal1 could modulate diverse repair processes. Based on previous research on its roles in the immune system and PNS, increased Gal1 expression after injury likely restricts inflammation and limits tissue damage. After peripheral nerve injury, high Gal1 levels in neurons and their axon's environment correlate with axon regeneration and functional recovery (McGraw et al., 2005; McGraw et al., 2004a), suggesting that increasing Gal1 within and around injured CNS neurons/axons could

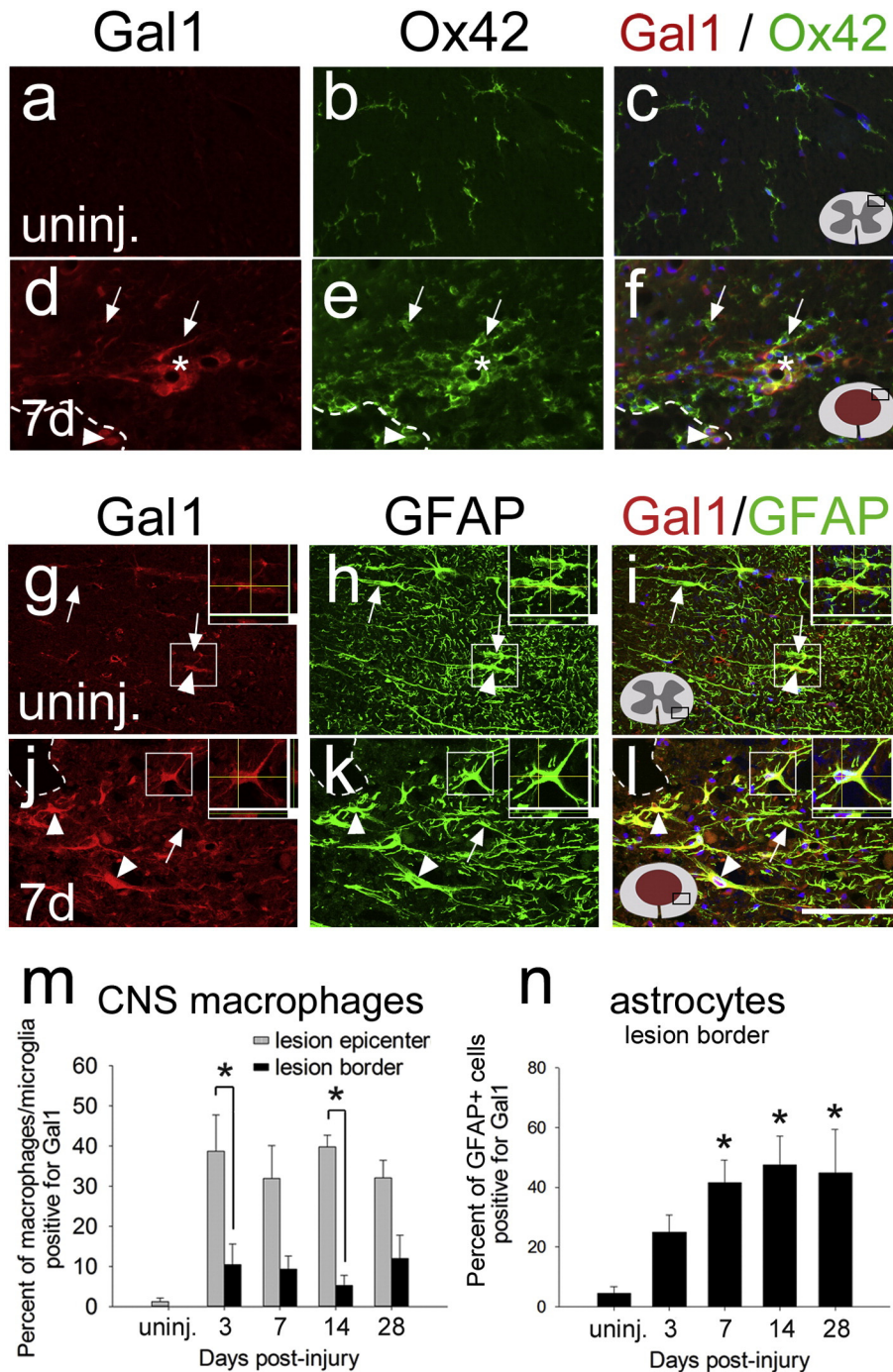


Fig. 5. In the lesion border, Gal1 was not strongly expressed by OX42+ microglia but was expressed by GFAP+ astrocytes. For all post-SCI images, the lesion is to the left of the image (dotted lines) and an area within the immediate lesion border is pictured (see schematic spinal cord for location). Arrows identify Gal1- cells; arrowheads show Gal1+ cells. Gal1 did not generally colocalize with OX42+ microglia in the uninjured spinal cord (a–c) or lesion border (d–f); however, Gal1 was often expressed by OX42+ amoeboid cells associated with blood vessels after SCI (asterisk, d–f). Gal1 colocalization with OX42+ cells was reduced in the lesion border compared to the epicenter (m). Although some GFAP+ astrocytes expressed Gal1 in the uninjured spinal cord (g–i), they strongly upregulated Gal1 by 7 dpi (j–l, n). In the lesion border, Gal1-IR was usually highest close to the lesion (glial scar) and decreased in a gradient moving away from the lesion. * $p < 0.05$. Scale bars = 100 μ m (large images), 25 μ m (insets).

improve repair. In the CNS, Gal1 upregulation can increase trophic factor release from astrocytes (Sasaki et al., 2004) and other cells, potentially improving axon growth and/or cell survival. In addition, Gal1 promotes neural stem cell proliferation (Sakaguchi et al., 2006; Yamane et al., 2010) and inhibits glutamate toxicity (Lekishvili et al., 2006). Furthermore, recent data indicate that exogenous Gal1 may enhance repair after SCI (Quinta et al., 2014). Additional research is needed to reveal whether supplementing endogenous Gal1 with recombinant Gal1 (e.g., gene therapy and direct injection) can modulate

neuroinflammation, restrict tissue damage, improve cell survival and growth, and promote functional recovery after SCI.

5. Experimental methods

5.1. Animals & surgery

All housing, surgery, and postoperative care conformed to The Ohio State University Institutional Animal Care and Use Committee guidelines.

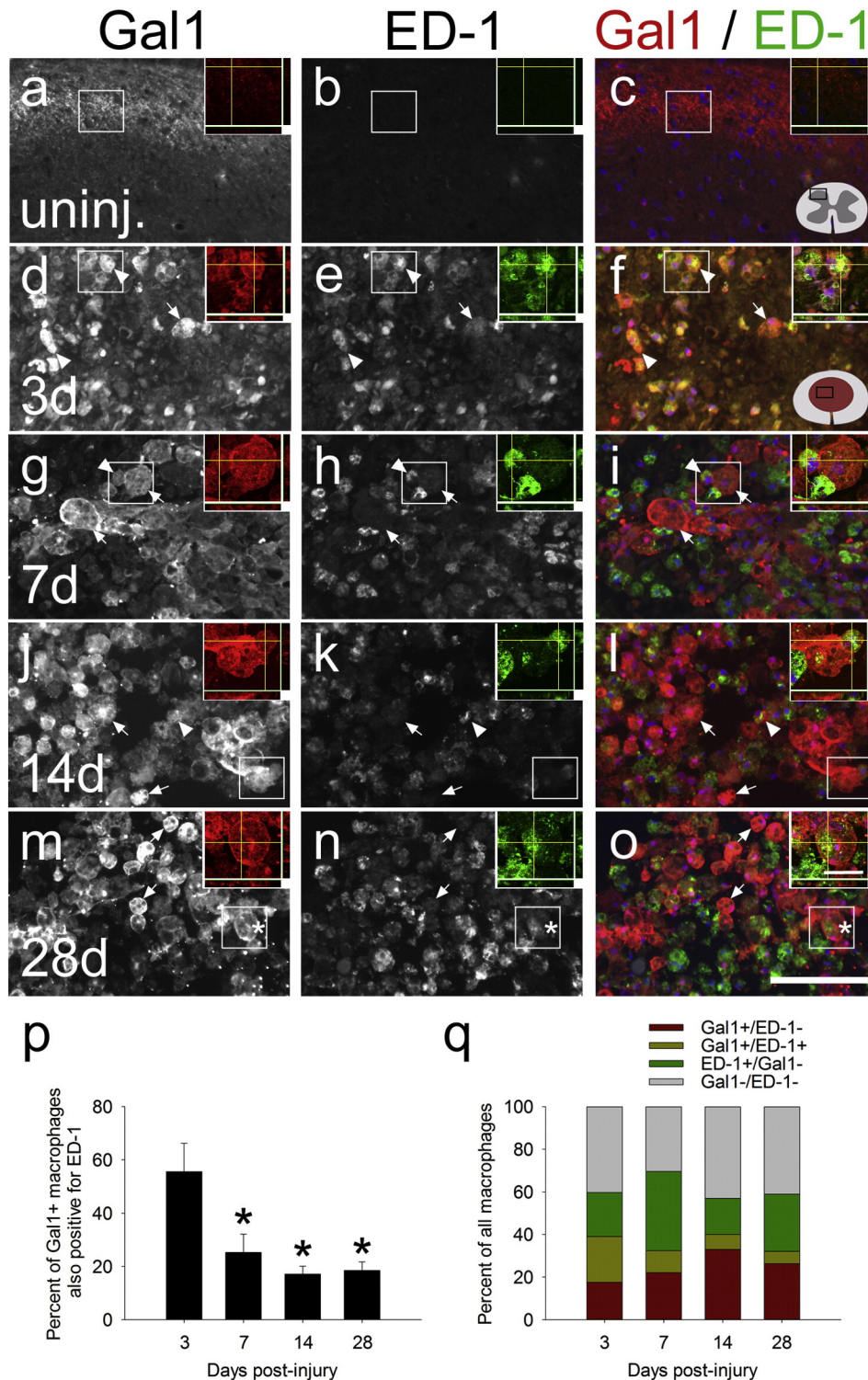


Fig. 6. Expression dynamics of the phagocytic marker ED1 within lesion-localized Gal1+ macrophages after SCI. For all panels, arrows specify Gal1+/ED1- macrophages; arrowheads identify Gal1+/ED1+ macrophages. Boxes in larger images are shown in confocal enlargements in insets. (a–c) ED1-IR cells were not observed in the uninjured spinal cord. (d–f) At 3 dpi, a high proportion of lesion-localized Gal1-IR macrophages also expressed ED1. (g–o) At later timepoints post-SCI, fewer Gal1-IR macrophages also contained ED1-IR. At these times, some large Gal1+/ED1- macrophages contained internal ED1+ compartments, presumably lysosomes (e.g., cell delineated by asterisk in m–o). (p) Quantification of the percent of Gal1-IR macrophages that also express ED1. (q) A representation of the Gal1+/ED1- (red), Gal1+/ED1+ (yellow), ED1+/Gal1- (green), and Gal1-/ED1- (gray) macrophage populations in the lesion site after injury. Note the reduced sizes of the yellow portions at 7–28 dpi compared to 3 dpi. * $p < 0.05$. Scale bars = 100 μ m (large images), 25 μ m (insets). (For interpretation of the references to color in this figure legend, the reader is referred to the web version of this article.)

All animals were fed standard chow and filtered tap water ad libitum and maintained on a 12:12 light/dark cycle. For all experiments, surgeries on rats from all timepoints were interspersed throughout the day (during the light cycle). Female Sprague–Dawley rats (200–250 g; 2–3 months

old; Harlan Laboratories) were anesthetized with an intraperitoneal injection of ketamine (80 mg/kg; obtained from Ohio State University Department of Pharmacy; JHP Pharmaceuticals) and xylazine (10 mg/kg; AnaSed, Lloyd Laboratories), and were treated with prophylactic

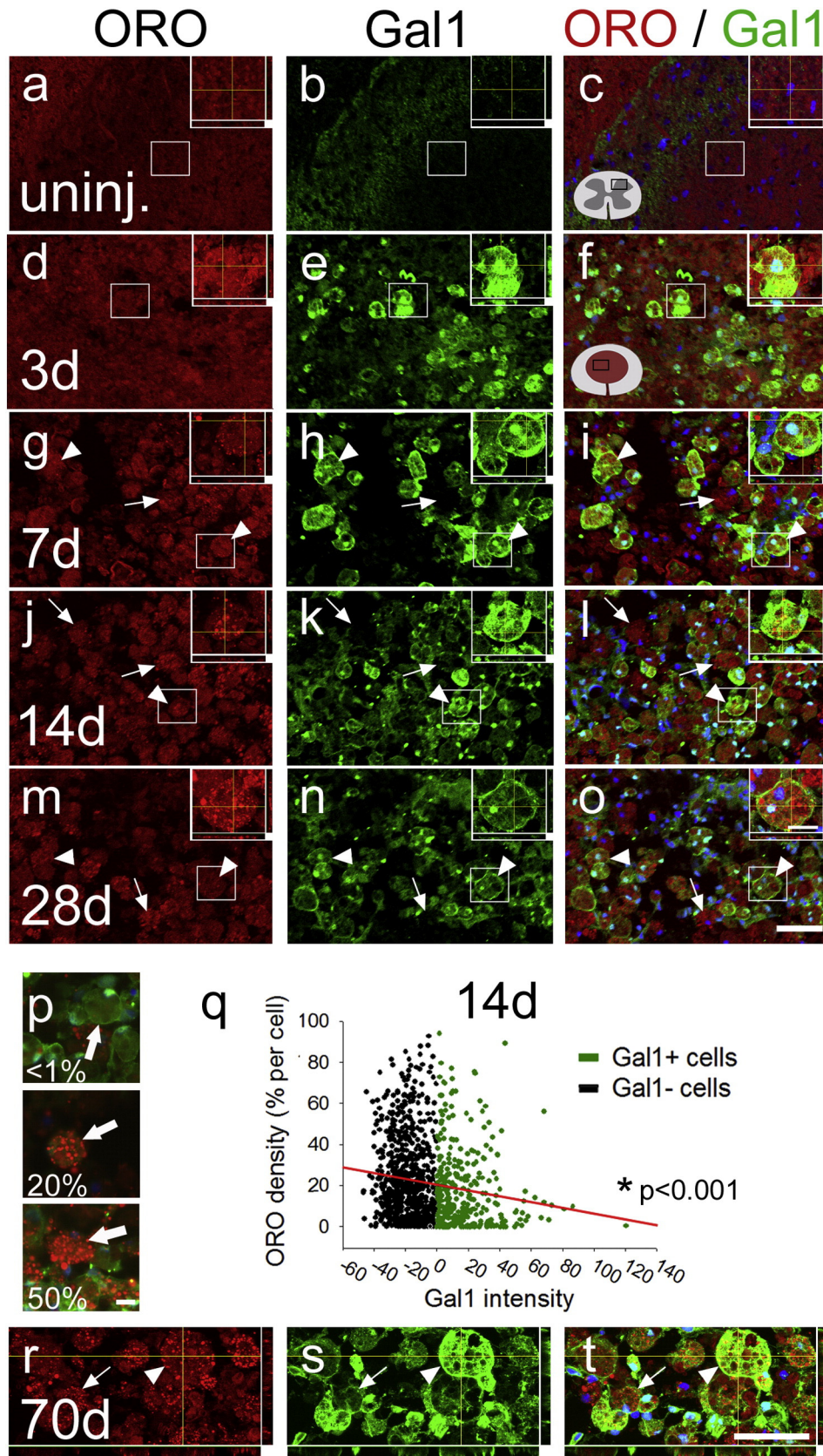


Fig. 7. At 14 d after SCI, lesion-localized macrophages that express Gal1 contain less phagocytosed lipids. Lipid-laden macrophages were identified by Oil Red O stain (ORO; red). Arrowheads identify Gal1 + / ORO-containing macrophages; arrows show Gal1 - / ORO-containing macrophages. (a–c) Uninjured spinal cord contained no detectable ORO stain. (d–o) After SCI, most macrophages in the lesion contained lipids. Both Gal1 + and Gal1 - macrophages were found to contain ORO stain. (p) Example images representing the quantification of ORO density within individually circled macrophages. The macrophages identified by the arrows had ORO densities of <1%, 20%, and 50% (top to bottom, respectively). (q) Regression analysis of the average percent ORO per cell in macrophages that were Gal1 + and Gal1 -. In individual macrophages from 14 dpi lesions, there was a significant negative correlation between Gal1 expression and ORO density. (r–t) Lipid-laden macrophages, some of which were Gal1 +, were found in the lesioned spinal cord even at chronic timepoints (70 dpi). Scale bars = 50 μm (large images), 5 μm (insets). (For interpretation of the references to color in this figure legend, the reader is referred to the web version of this article.)

antibiotics (gentamicin sulfate (Butler Schein), 1.25 mg s.c. in 0.25 mL sterile water). A partial T8 laminectomy was performed prior to SCI. The periosteum, but not the dura, was removed for all surgeries. Animals were subjected to a moderate contusion injury (200 kDyn) using the Infinite Horizons device (Precision Systems and Instrumentation). Post-operative animal care included daily administration of gentamicin (1 mL/d for 5 d), subcutaneous injection of Ringer's solution (5, 5, 4, 3, 2 mL on the first 5 dpi, respectively) to prevent dehydration, and manual voiding of bladders twice daily. Urine pH was assessed weekly and animals were monitored daily for infection or other signs of suboptimal recovery. Rats used in the immunohistochemistry timecourse study survived for 3 ($n = 4$), 7 ($n = 5$), 14 ($n = 4$), or 28 days ($n = 4$), and tissue from uninjured control animals ($n = 5$) was collected at the same time (all animals received SCI on the same day; one uninjured animal was dissected at each timepoint plus an extra uninjured animal with the 28 dpi cohort).

5.2. Western blots

Protein samples were derived from injured rat spinal cords (175 kDyn injury; T8 spinal level; 5 mm tissue segments centered on the injury site). (Samples were from our laboratory's prepared tissue bank, hence the different injury severity from the rat SCI timecourse above.) Spinal cord segments were removed then digested in T-PER (tissue protein extraction reagent; Pierce 78510). Sample protein concentrations were assessed using Coomassie Plus Protein Assay Kit (Pierce 23236). 20 μ g protein from each sample was diluted in NuPAGE LDS sample buffer (Life Technologies NP0008) before being loaded into a 4–12% Bis-Tris gel (Life Technologies NP0336BOX) and run for 45 min at 200 V. Proteins were transferred to a nitrocellulose membrane (Biorad 162-01115) for 80 min at 30 V. The membrane was blocked with 5% bovine serum albumin (Fisher BP1600) for 45 min then incubated with primary antibody (goat anti-galactin-1 (1:1000; R&D Systems AF1245); rat anti- α -tubulin (1:80,000; Serotec MCA77G)) overnight at 4 °C. The next day, the membrane was washed 3 times with PBS/Tween20 before incubating the membrane with secondary antibodies: horse radish peroxidase (HRP)-conjugated rabbit anti-goat (1:1000; Jackson 305-035-003) and goat anti-rat (1:1000; Jackson 115-035-174). Detection of α -tubulin was used as a loading control. A chemiluminescent HRP substrate kit (Pierce 34078) was used to develop the blot, and the membrane was imaged and analyzed on Kodak Image Station 4000MM PRO. For all SCI groups, $n = 3$. No differences were observed between naïve uninjured ($n = 3$) and 7 days post-laminectomy (sham-injured) controls ($n = 3$), so these samples were pooled.

5.3. mRNA processing and PCR

RNA for quantitative real-time (qRT)-PCR was isolated from SCI animals as described previously (Kigerl et al., 2007). Gene primer pairs (Life Technologies custom primers: Gal1 F: CGCCAAGAGCTTTGTGTTGA; Gal1 R: GGCAGTCTCCCGTTGTTCTG) were used to assay mRNA levels in uninjured and SCI spinal cords (uninjured: $n = 3$; all other groups: $n = 4$). For all samples, expression was normalized to 18S rRNA. mRNA expression is shown relative to control (uninjured spinal cord).

5.4. Tissue processing and immunohistochemistry

Animals were anesthetized with an overdose of ketamine/xylazine and perfused intracardially with PBS (0.1 M, pH 7.4) followed by 4% paraformaldehyde in 0.1% PB. Fixed spinal cords were placed in 4% paraformaldehyde overnight then switched to 20% sucrose the next day prior to tissue blocking. A 1 cm length of spinal cord, centered on the injury site, was flash frozen in OCT compound to prepare tissue for cryosectioning. Spinal cord tissue was sectioned at 10 μ m transversely and stored at -80 °C. Spinal cords from different timepoints or treatment

groups were distributed across blocks and coded to ensure uniformity of staining and to ensure that analysis was performed in a blind manner. For immunohistochemistry, slides were washed with 0.1 M PBS before applying a blocking solution (10% normal goat serum or 10% normal donkey serum, depending on secondary used) for 45 min. Primary antibody (in 0.1 M PBS + 0.2% Triton-X) was applied overnight (goat anti-galactin-1, 1:400, R&D Systems BAF1245; mouse anti-OX42, 1:1000, Serotec MCA275; rabbit anti-Iba1, 1: 1000, Wako 019–19741; mouse anti-ED1, 1:2000, Serotec MCA341R; rabbit anti-GFAP, 1:20,000, Dako Z0334). The next day, slides were washed 3 times with PBS then secondary antibodies (1:500 in PBS/0.2% Triton-X) were added for 2 h: (Alexa 546-conjugated goat anti-rat (A11081), goat-anti-mouse (A11030), and donkey anti-goat (A11056); or 488-conjugated goat anti-rabbit (A11034) and goat anti-mouse (A11001); all from Life Technologies). Slides were washed with PBS, stained with DAPI nuclear stain for 5 min then washed once more before coverslipping with Immu-Mount (Thermo Scientific 9990402).

5.5. Image analysis: Gal1-IR in macrophages & astrocytes after SCI

To measure overall level of Gal1-IR after SCI, spinal cord cross-sections cut at the epicenter, and at 1.0 and 1.4 mm rostral and caudal to the lesion epicenter at various timepoints were stained for Gal1 after which digital montages were created. Samples at 3 dpi were not analyzed, since the lesion had not consolidated at this time. Images were analyzed using MetaMorph: the area of interest (spared tissue, lesioned tissue, or both) was manually identified and a threshold was applied to define Gal1 + areas, thereby allowing Gal1-IR density to be calculated as a percent of total area.

For OX42-Gal1 co-localization analysis, OX42-IR amoeboid macrophages in the lesion site were identified and circled using MetaMorph (at least 1000 cells per animal). The overlay with circles was superimposed on the corresponding Gal1 image and the area and average Gal1-IR intensity of each circled macrophage were measured. For comparison, Gal1-IR intensity in microglia from uninjured tissue (and in the parenchyma adjacent to lesion) was analyzed. Since microglia were intensely OX42-IR and did not overlap with other microglia within a section, automated thresholds were used (rather than cell circling) to identify labeled microglia. This overlay was then superimposed onto the corresponding Gal1 image and average Gal1-IR was measured. For all analyses, two slightly Gal1-negative cells (right at background staining levels) and two slightly Gal1-positive cells (just above background levels) were circled to define the threshold for Gal1 positivity in each individual image (threshold set to 0 Gal1-IR intensity). Data are expressed as percent of macrophages/microglia positive for Gal1.

For GFAP-Gal1 co-localization analysis, thresholds were applied and images were analyzed as described for microglia above. Thresholds were applied on the GFAP image to identify GFAP-IR cells and processes, then the overlay was transferred to the corresponding Gal1 image to define Gal1-IR intensity in GFAP + cells/processes. Areas < 50 pixels squared were excluded to remove GFAP-IR specks or small processes. Positive Gal1-IR was defined as described above and data expressed as percent of GFAP + cells/processes that were also positively labeled with Gal1.

For ED-1-Gal1 co-localization analysis, thresholds were applied for Gal1 and ED1 as described above. Gal1 + cells were circled, the overlay was transferred to the ED1 image, and average intensity of ED1-IR was measured. The percent of Gal1 + cells that also contained above-threshold ED1-IR was calculated. For ORO analysis, ORO density per cell was measured by circling individual cells, thresholding the ORO channel for positivity, then taking the percent area per cell that was ORO +.

5.6. Statistics

Immunohistologic, morphometric, Western, and gene expression data were analyzed using one- or two-way ANOVA, followed by Holm–Sidak

post-hoc test. The Gal1–ORO relationship was analyzed using Pearson correlation. SigmaPlot 12.0 (SPSS) and InStat 3 (GraphPad, La Jolla, CA) were used to analyze the data. Data were considered significant when $p < 0.05$. All data are plotted as mean \pm SEM.

Acknowledgments

The authors thank Dr Kristina Kigerl for assisting with techniques and equipment, Dr Andrew Sauerbeck for editorial advice, and Lori Hudson and Wenmin Lai for their technical expertise. Ohio State University's Campus Microscopy & Imaging Facility (CMIF) and Nucleic Acid Shared Resource provided facilities for confocal microscopy and qPCR analysis, respectively. This work was supported by a Canadian Institutes of Health Research (CIHR) Postdoctoral Fellowship (ADG), the Ray W. Poppleton Endowment (PGP), and National Institutes of Health Grant R01NS072304 (PGP).

References

- Akazawa, C., Nakamura, Y., Sango, K., Horie, H., Kohsaka, S., 2004. Distribution of the galectin-1 mRNA in the rat nervous system: its transient upregulation in rat facial motor neurons after facial nerve axotomy. *Neuroscience* 125, 171–178.
- Barriounevo, P., Beigier-Bompadre, M., Ilarregui, J.M., Toscano, M.A., Bianco, G.A., Isturiz, M.A., Rabinovich, G.A., 2007. A novel function for galectin-1 at the crossroad of innate and adaptive immunity: galectin-1 regulates monocyte/macrophage physiology through a nonapoptotic ERK-dependent pathway. *J. Immunol.* 178, 436–445.
- Camby, I., Le, M.M., Lefranc, F., Kiss, R., 2006. Galectin-1: a small protein with major functions. *Glycobiology* 16, 137R–157R.
- Carrico, K.M., Vaishnav, R., Hall, E.D., 2009. Temporal and spatial dynamics of peroxynitrite-induced oxidative damage after spinal cord contusion injury. *J. Neurotrauma* 26, 1369–1378.
- Correa, S.G., Sotomayor, C.E., Aoki, M.P., Maldonado, C.A., Rabinovich, G.A., 2003. Opposite effects of galectin-1 on alternative metabolic pathways of L-arginine in resident, inflammatory, and activated macrophages. *Glycobiology* 13, 119–128.
- Damoiseau, J.G., Dopp, E.A., Calame, W., Chao, D., MacPherson, G.G., Dijkstra, C.D., 1994. Rat macrophage lysosomal membrane antigen recognized by monoclonal antibody ED1. *Immunology* 83, 140–147.
- Donnelly, D.J., Popovich, P.G., 2008. Inflammation and its role in neuroprotection, axonal regeneration and functional recovery after spinal cord injury. *Exp. Neurol.* 209, 378–388.
- Echigo, Y., Sugiki, H., Koizumi, Y., Hikitsuchi, S., Inoue, H., 2010. Activation of RAW264.7 macrophages by oxidized galectin-1. *Immunol. Lett.* 131, 19–23.
- Fukaya, K., Hasegawa, M., Mashitani, T., Kadoya, T., Horie, H., Hayashi, Y., Fujisawa, H., Tachibana, O., Kida, S., Yamashita, J., 2003. Oxidized galectin-1 stimulates the migration of Schwann cells from both proximal and distal stumps of transected nerves and promotes axonal regeneration after peripheral nerve injury. *J. Neuropathol. Exp. Neurol.* 62, 162–172.
- Gaudet, A.D., Steeves, J.D., Tetzlaff, W., Ramer, M.S., 2005. Expression and functions of galectin-1 in sensory and motoneurons. *Curr. Drug Targets* 6, 419–425.
- Gaudet, A.D., Leung, M., Poirier, F., Kadoya, T., Horie, H., Ramer, M.S., 2009. A role for galectin-1 in the immune response to peripheral nerve injury. *Exp. Neurol.* 220, 320–327.
- Gaudet, A.D., Popovich, P.G., Ramer, M.S., 2011. Wallerian degeneration: gaining perspective on inflammatory events after peripheral nerve injury. *J. Neuroinflammation* 8, 110.
- Greenhalgh, A.D., David, S., 2014. Differences in the phagocytic response of microglia and peripheral macrophages after spinal cord injury and its effects on cell death. *J. Neurosci.* 34, 6316–6322.
- Han, H., Xia, Y., Wang, S., Zhao, B., Sun, Z., Yuan, L., 2011. Synergistic effects of galectin-1 and reactive astrocytes on functional recovery after contusive spinal cord injury. *Arch. Orthop. Trauma Surg.* 131, 829–839.
- Herbert, D.R., Holscher, C., Mohrs, M., Arendse, B., Schwegmann, A., Radwanska, M., Leeto, M., Kirsch, R., Hall, P., Mossmann, H., Clausen, B., Forster, I., Brombacher, F., 2004. Alternative macrophage activation is essential for survival during schistosomiasis and downmodulates T helper 1 responses and immunopathology. *Immunity* 20, 623–635.
- Holness, C.L., Simmons, D.L., 1993. Molecular cloning of CD68, a human macrophage marker related to lysosomal glycoproteins. *Blood* 81, 1607–1613.
- Horie, H., Kadoya, T., Hikawa, N., Sango, K., Inoue, H., Takeshita, K., Asawa, R., Hiroi, T., Sato, M., Yoshioka, T., Ishikawa, Y., 2004. Oxidized galectin-1 stimulates macrophages to promote axonal regeneration in peripheral nerves after axotomy. *J. Neurosci.* 24, 1873–1880.
- Inagaki, Y., Sohma, Y., Horie, H., Nozawa, R., Kadoya, T., 2000. Oxidized galectin-1 promotes axonal regeneration in peripheral nerves but does not possess lectin properties. *Eur. J. Biochem.* 267, 2955–2964.
- Ishibashi, S., Kuroiwa, T., Sakaguchi, M., Sun, L., Kadoya, T., Okano, H., Mizusawa, H., 2007. Galectin-1 regulates neurogenesis in the subventricular zone and promotes functional recovery after stroke. *Exp. Neurol.* 207, 302–313.
- Kigerl, K.A., Lai, W., Rivest, S., Hart, R.P., Satoskar, A.R., Popovich, P.G., 2007. Toll-like receptor (TLR)-2 and TLR-4 regulate inflammation, gliosis, and myelin sparing after spinal cord injury. *J. Neurochem.* 102, 37–50.
- Kigerl, K.A., Gensel, J.C., Ankeny, D.P., Alexander, J.K., Donnelly, D.J., Popovich, P.G., 2009. Identification of two distinct macrophage subsets with divergent effects causing either neurotoxicity or regeneration in the injured mouse spinal cord. *J. Neurosci.* 29, 13435–13444.
- Kurihara, D., Ueno, M., Tanaka, T., Yamashita, T., 2010. Expression of galectin-1 in immune cells and glial cells after spinal cord injury. *Neurosci. Res.* 66, 265–270.
- Lee, S., Huen, S., Nishio, H., Nishio, S., Lee, H.K., Choi, B.S., Ruhrberg, C., Cantley, L.G., 2011. Distinct macrophage phenotypes contribute to kidney injury and repair. *J. Am. Soc. Nephrol.* 22, 317–326.
- Lekishvili, T., Hesketh, S., Brazier, M.W., Brown, D.R., 2006. Mouse galectin-1 inhibits the toxicity of glutamate by modifying NR1 NMDA receptor expression. *Eur. J. Neurosci.* 24, 3017–3025.
- Liu, D., Shan, Y., Valluru, L., Bao, F., 2013. Mn (III) tetrakis (4-benzoic acid) porphyrin scavenges reactive species, reduces oxidative stress, and improves functional recovery after experimental spinal cord injury in rats: comparison with methylprednisolone. *BMC Neurosci.* 14, 23.
- Martinez, F.O., Helming, L., Gordon, S., 2009. Alternative activation of macrophages: an immunological functional perspective. *Annu. Rev. Immunol.* 27, 451–483.
- Martini, R., Fischer, S., Lopez-Vales, R., David, S., 2008. Interactions between Schwann cells and macrophages in injury and inherited demyelinating disease. *Glia* 56, 1566–1577.
- McGraw, J., McPhail, L.T., Oschipok, L.W., Horie, H., Poirier, F., Steeves, J.D., Ramer, M.S., Tetzlaff, W., 2004a. Galectin-1 in regenerating motoneurons. *Eur. J. Neurosci.* 20, 2872–2880.
- McGraw, J., Oschipok, L.W., Liu, J., Hiebert, G.W., Mak, C.F., Horie, H., Kadoya, T., Steeves, J.D., Ramer, M.S., Tetzlaff, W., 2004b. Galectin-1 expression correlates with the regenerative potential of rubrospinal and spinal motoneurons. *Neuroscience* 128, 713–719.
- McGraw, J., Gaudet, A.D., Oschipok, L.W., Kadoya, T., Horie, H., Steeves, J.D., Tetzlaff, W., Ramer, M.S., 2005. Regulation of neuronal and glial galectin-1 expression by peripheral and central axotomy of rat primary afferent neurons. *Exp. Neurol.* 195, 103–114.
- McPhail, L.T., Stirling, D.P., Tetzlaff, W., Kwicien, J.M., Ramer, M.S., 2004. The contribution of activated phagocytes and myelin degeneration to axonal retraction/dieback following spinal cord injury. *Eur. J. Neurosci.* 20, 1984–1994.
- Miron, V.E., Boyd, A., Zhao, J.W., Yuen, T.J., Ruckh, J.M., Shadrach, J.L., van, W.P., Wagers, A.J., Williams, A., Franklin, R.J., Ffrench-Constant, C., 2013. M2 microglia and macrophages drive oligodendrocyte differentiation during CNS remyelination. *Nat. Neurosci.* 16, 1211–1218.
- Moiseeva, E.P., Williams, B., Samani, N.J., 2003. Galectin 1 inhibits incorporation of vitronectin and chondroitin sulfate B into the extracellular matrix of human vascular smooth muscle cells. *Biochim. Biophys. Acta* 1619, 125–132.
- Mosser, D.M., Edwards, J.P., 2008. Exploring the full spectrum of macrophage activation. *Nat. Rev. Immunol.* 8, 958–969.
- Outenreath, J.L., Jones, A.L., 1992. Influence of an endogenous lectin substrate on cultured dorsal root ganglion cells. *J. Neurocytol.* 21, 788–795.
- Pesce, J.T., Ramalingam, T.R., Mentink-Kane, M.M., Wilson, M.S., El Kasmi, K.C., Smith, A.M., Thompson, R.W., Cheever, A.W., Murray, P.J., Wynn, T.A., 2009. Arginase-1-expressing macrophages suppress Th2 cytokine-driven inflammation and fibrosis. *PLoS Pathog.* 5, e1000371.
- Plachta, N., Annaheim, N., Bissière, S., Lin, S., Rüegg, M., Hoving, S., Müller, D., Poirier, F., Bibel, M., Barde, Y.A., 2007. Identification of a lectin causing the degeneration of neuronal processes using engineered embryonic stem cells. *Nat. Neurosci.* 10, 712–719.
- Popovich, P.G., Wei, P., Stokes, B.T., 1997. Cellular inflammatory response after spinal cord injury in Sprague–Dawley and Lewis rats. *J. Comp. Neurol.* 377, 443–464.
- Pruss, H., Kopp, M.A., Brommer, B., Gatzemeier, N., Laginha, I., Dirnagl, U., Schwab, J.M., 2011. Non-resolving aspects of acute inflammation after spinal cord injury (SCI): indices and resolution plateau. *Brain Pathol.* 21, 652–660.
- Qu, W.S., Wang, Y.H., Wang, J.P., Tang, Y.X., Zhang, Q., Tian, D.S., Yu, Z.Y., Xie, M.J., Wang, W., 2010. Galectin-1 enhances astrocytic BDNF production and improves functional outcome in rats following ischemia. *Neurochem. Res.* 35, 1716–1724.
- Qu, W.S., Wang, Y.H., Ma, J.F., Tian, D.S., Zhang, Q., Pan, D.J., Yu, Z.Y., Xie, M.J., Wang, J.P., Wang, W., 2011. Galectin-1 attenuates astrogliosis-associated injuries and improves recovery of rats following focal cerebral ischemia. *J. Neurochem.* 116, 217–226.
- Quinta, H.R., Pasquini, J.M., Rabinovich, G.A., Pasquini, L.A., 2014. Glycan-dependent binding of galectin-1 to neuropilin-1 promotes axonal regeneration after spinal cord injury. *Cell Death Differ.* 21, 941–955.
- Rabinovich, G.A., Sotomayor, C.E., Riera, C.M., Bianco, I., Correa, S.G., 2000. Evidence of a role for galectin-1 in acute inflammation. *Eur. J. Immunol.* 30, 1331–1339.
- Rabinovich, G.A., Liu, F.T., Hirashima, M., Anderson, A., 2007. An emerging role for galectins in tuning the immune response: lessons from experimental models of inflammatory disease, autoimmunity and cancer. *Scand. J. Immunol.* 66, 143–158.
- Sakaguchi, M., Shingo, T., Shimazaki, T., Okano, H.J., Shiwa, M., Ishibashi, S., Oguro, H., Ninomiya, M., Kadoya, T., Horie, H., Shibuya, A., Mizusawa, H., Poirier, F., Nakauchi, H., Sawamoto, K., Okano, H., 2006. A carbohydrate-binding protein, Galectin-1, promotes proliferation of adult neural stem cells. *Proc. Natl. Acad. Sci. U. S. A.* 103, 7112–7117.
- Sasaki, T., Hirabayashi, J., Many, H., Kasai, K., Endo, T., 2004. Galectin-1 induces astrocyte differentiation, which leads to production of brain-derived neurotrophic factor. *Glycobiology* 14, 357–363.
- Stancic, M., van, H.J., Thijsen, V.L., Gabius, H.J., van, D.V., Hoekstra, D., Baron, W., 2011. Increased expression of distinct galectins in multiple sclerosis lesions. *Neuropathol. Appl. Neurobiol.* 37, 654–671.

- Stirling, D.P., Khodarahmi, K., Liu, J., McPhail, L.T., McBride, C.B., Steeves, J.D., Ramer, M.S., Tetzlaff, W., 2004. Minocycline treatment reduces delayed oligodendrocyte death, attenuates axonal dieback, and improves functional outcome after spinal cord injury. *J. Neurosci.* 24, 2182–2190.
- Tamatani, T., Kotani, M., Miyasaka, M., 1991. Characterization of the rat leukocyte integrin, CD11/CD18, by the use of LFA-1 subunit-specific monoclonal antibodies. *Eur. J. Immunol.* 21, 627–633.
- Thomas, A.C., Sala-Newby, G.B., Ismail, Y., Johnson, J.L., Pasterkamp, G., Newby, A.C., 2007. Genomics of foam cells and nonfoamy macrophages from rabbits identifies arginase-I as a differential regulator of nitric oxide production. *Arterioscler. Thromb. Vasc. Biol.* 27, 571–577.
- Vallieres, N., Berard, J.L., David, S., Lacroix, S., 2006. Systemic injections of lipopolysaccharide accelerates myelin phagocytosis during Wallerian degeneration in the injured mouse spinal cord. *Glia* 53, 103–113.
- Yamane, J., Nakamura, M., Iwanami, A., Sakaguchi, M., Katoh, H., Yamada, M., Momoshima, S., Miyao, S., Ishii, K., Tamaoki, N., Nomura, T., Okano, H.J., Kanemura, Y., Toyama, Y., Okano, H., 2010. Transplantation of galectin-1-expressing human neural stem cells into the injured spinal cord of adult common marmosets. *J. Neurosci. Res.* 88, 1394–1405.
- Yin, P., Knolhoff, A.M., Rosenberg, H.J., Millet, L.J., Gillette, M.U., Sweedler, J.V., 2012. Peptidomic analyses of mouse astrocytic cell lines and rat primary cultured astrocytes. *J. Proteome Res.* 11, 3965–3973.